

Observational Limit on Gravitational Waves from Binary Neutron Stars in the Galaxy

B. Allen,¹ J. K. Blackburn,² P. R. Brady,³ J. D. E. Creighton,^{1,4} T. Creighton,⁴ S. Droz,⁵ A. D. Gillespie,² S. A. Hughes,⁴ S. Kawamura,² T. T. Lyons,² J. E. Mason,² B. J. Owen,⁴ F. J. Raab,² M. W. Regehr,² B. S. Sathyaprakash,⁶ R. L. Savage, Jr.,² S. Whitcomb,² and A. G. Wiseman¹

¹*Department of Physics, University of Wisconsin-Milwaukee, P.O. Box 413, Milwaukee, Wisconsin 53201*

²*LIGO Project, MS 18-34, California Institute of Technology, Pasadena, California 91125*

³*Institute for Theoretical Physics, University of California, Santa Barbara, California 93106*

⁴*Theoretical Astrophysics 130-33, California Institute of Technology, Pasadena, California 91125*

⁵*Department of Physics, University of Guelph, Guelph, Ontario, Canada N1G 2W1*

⁶*Department of Physics and Astronomy, UWCC, Post Box 913, Cardiff CF2 3YB, Wales*

(Received 31 March 1999)

Using optimal matched filtering, we search 25 hours of data from the LIGO 40-m prototype laser interferometric gravitational-wave detector for gravitational-wave chirps emitted by coalescing binary systems within our Galaxy. This is the first test of this filtering technique on real interferometric data. An upper limit on the rate R of neutron star binary inspirals in our Galaxy is obtained: with 90% confidence, $R < 0.5 \text{ h}^{-1}$. Similar experiments with LIGO interferometers will provide constraints on the population of tight binary neutron star systems in the Universe.

PACS numbers: 95.85.Sz, 04.80.Nn, 07.05.Kf, 97.80.-d

A worldwide effort is underway to test a fundamental prediction of physics (the existence of gravitational waves) using a new generation of gravitational-wave detectors capable of making astrophysical observations. These efforts include the US Laser Interferometer Gravitational-wave Observatory (LIGO) [1], VIRGO (French/Italian) [2], GEO-600 (British/German) [2], TAMA (Japanese) [2], and ACIGA (Australian) [3]. The detectors are laser interferometers with a beam splitter and mirrors suspended on wires. A gravitational wave displaces the mirrors, and shifts the relative optical phase in two perpendicular paths. This causes a shift in the interference pattern at the beam splitter [4]. Within the next decade, these facilities should be sensitive enough to observe gravitational waves from astrophysical sources at distances of tens to hundreds of megaparsecs (Mpc).

During the past 15 years, the LIGO project has used a 40-m prototype interferometer at Caltech to develop optical and control elements for the full-scale detectors under construction in Hanford, Washington, and Livingston, Louisiana [5]. In 1994, this instrument was configured as a modulated Fabry-Perot interferometer: light returning from the two arms was independently sensed [6]. In this configuration, the detector had its best differential displacement sensitivity of $\approx 3.5 \times 10^{-19} \text{ m Hz}^{-1/2}$ over a bandwidth of approximately a kHz centered at 600 Hz.

A week-long test run of the instrument was made in November 1994 prior to a major reconfiguration. Figure 1 shows the data-taking periods. The run yielded 44.8 hours of tape; both arms were in optical resonance for 39.9 hours (89% of the time). Although the data was taken for diagnostic purposes, it provides an excellent opportunity to obtain observational limits on gravitational-wave sources, and to examine analysis techniques.

A major challenge arises because the real detector noise does not satisfy the usual simplifying assumptions: stationary and Gaussian. The 40-m data have the expected colored broadband background but with significant deterministic components (spectral peaks), including $\sim 10^2$ sinusoidal components arising from the vibration of the

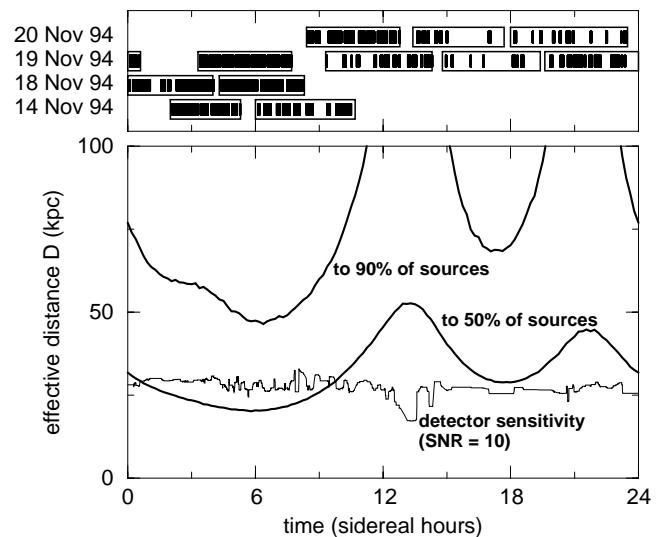


FIG. 1. Top: boxes show data collection times. Dark bars show data actually filtered. Bottom: effective distance D [Eq. (1)] to 90% (50%) of sources varies as the detector antenna pattern sweeps past the Galactic center. The dip at 6 h is when the nadir of the detector (turning with the Earth) points closest to the Galactic center where the potential sources are clustered. Fortunately, much of the data was taken near such times. Jagged line: effective distance D at which a $2 \times 1.4 M_{\odot}$ optimally oriented coalescing system would give $\text{SNR} = \rho = 10$. This depends on the average sensitivity of the instrument. The small fluctuations indicate stable sensitivity.

support wires and 60 Hz line harmonics. There are also transient features occurring every few minutes: bursts of noise with durations of ~ 1 –500 ms from accidental (natural or man-made) disturbances. These difficulties led us to develop data analysis techniques that make matched filtering methods perform well on real data.

This Letter reports on a search of these data for binary inspiral chirps—the gravitational waveforms produced by pairs of orbiting stars or black holes. The search focuses on neutron star binaries in our Galaxy. On time scales of $\approx 10^7$ yr a binary loses energy by emitting gravitational waves (primarily at twice the orbital frequency). As the orbit shrinks, it circularizes and the period decreases. We search for the gravitational waves that would be emitted during the final few seconds of this process; the stars orbit hundreds of times per second at separations of tens of km before plunging together. (See [5] for results of preliminary searches.)

The data stream was searched using *matched filtering*. This method [7] uses linear filters constructed from the expected waveforms, computed using the second post-Newtonian approximation (2PN) [8]. The 2PN waveform for a $2 \times 1.4M_\odot$ binary is a sweeping sinusoid which enters the detector passband at about 120 Hz. The frequency and amplitude increase during the ensuing 255 cycles; after 1.35 s the frequency has increased to 1822 Hz and the waveform is cut off when the stars merge. The 2PN approximation results in a reduction of signal-to-noise ratio (SNR) $< 10\%$ [9].

The dimensionless strain $h(t)$ of the gravitational wave produces a differential change $\Delta L(t) = Lh(t)$ in the lengths of the two perpendicular interferometer arms [4], where $L = 38.25$ m is the average arm length. For a binary system (circular orbits, no spin) with masses $M = (m_1, m_2)$ this strain is

$$h(t) = \frac{1 \text{ Mpc}}{D} [\sin\alpha h_s^M(t - t_0) + \cos\alpha h_c^M(t - t_0)]. \quad (1)$$

Here α is a constant determined by the orbital phase and orientation of the binary system, t_0 is the laboratory time when the chirp signal first enters the detector passband, and $h_{s,c}^M(t - t_0)$ are the two polarizations of the gravitational waveform produced by an inspiraling binary system that is *optimally oriented* at 1 Mpc. If x, y axes are defined by the two interferometer arms, then an *optimally oriented* binary system is located on the z axis with its orbital plane parallel to the x - y plane. The effective distance D depends on the distance to the source and on its orientation with respect to the detector. The detector has a nonuniform response over the sky due to its quadrupolar antenna pattern. If the source is not optimally oriented (i.e., not on the z axis or the orbital plane is tipped), then D is greater than the source-detector distance. The formulas for $h_{s,c}^M$ are Eqs. (2,3a,4a) of Ref. [8].

The detector signal is the voltage applied to produce a feedback force on the mirrors to hold the interferome-

ter in resonance; it is proportional to the differential displacement $\Delta L(t)$. This voltage $v(t)$ was recorded at a sample rate of 9868.42 Hz by a 12 bit analog-to-digital converter. Quantizing the data reduces the SNR by less than 0.9% [10]. The instrument's frequency and phase response $\tilde{R}(f)$ was determined at the beginning of each of eleven ~ 4 h data runs by applying known perturbative forces to the interferometer [11]. These eleven calibration curves differ by less than 5%. Because errors in calibration affect the SNR only at second order, we estimate the effects of any calibration errors or drifts on SNR to be less than 0.3%. The voltage output $v_h(t)$ that would be produced by a binary inspiral is given by

$$\begin{aligned} v_h(t) &= \int_{-\infty}^t R(t - t')h(t') dt' \\ &= \int_{-\infty}^{\infty} \tilde{h}(f)\tilde{R}^*(f)e^{-2\pi ift} df, \end{aligned}$$

where $Q(t)$ and $\tilde{Q}(f)$ denote Fourier transform pairs.

We search for inspiral waveforms using (digital) matched filtering. Because the inspiral waveforms depend upon the source masses $M = (m_1, m_2)$, we use a “bank” of template waveforms with masses spaced closely enough [12] to detect any signal in the mass range $1.0M_\odot < m_1, m_2 < 3.0M_\odot$ [13]. The bank contains 687 filters M_k and is designed so that no more than 2% of SNR would be lost if the mass parameters M of a signal did not exactly match one of the M_k . For each mass pair M_k in the template bank, two real signals are constructed:

$$X_k^{s,c}(t) = N_k^{s,c} \int_{-\infty}^{\infty} \frac{\tilde{v}(f)\tilde{h}_{s,c}^{*M_k}\tilde{R}(f)}{S_v(|f|)} e^{-2\pi ift} df. \quad (2)$$

These are the outputs of optimal filters matched to the waveform of the k th mass pair M_k . The denominator $S_v(|f|)$ is (an estimate of) the one-sided power spectral density of $v(t)$; if the detector's noise is stationary and Gaussian, then these filters are optimal. The normalization factor $N_k^{s,c}$ is chosen so that, in the absence of any signals, the mean value of $[X_k^{s,c}(t)]^2$ is unity. We define the SNR for the k th template waveform to be

$$\rho_k(t) = \text{SNR} = \sqrt{[X_k^s(t)]^2 + [X_k^c(t)]^2},$$

arrived at by maximizing over the phase α of the binary system. The effective distance D at which coalescence of $2 \times 1.4M_\odot$ stars would yield a SNR of 10 in the interferometer is shown in Fig. 1. (The definition of the SNR follows Ref. [12] and other literature. Its expected value for a source scales $\propto D^{-1}$. Its rms value for a single template is $\sqrt{2}$ in the presence of Gaussian noise alone.)

The data was processed, using fast-Fourier transform (FFT) methods, in overlapping ≈ 26.6 s *segments* (2^{18} samples). To avoid end effects, $S_v^{-1}(|f|)$ in Eq. (2) was truncated at ≈ 13.3 s in the time domain. The longest chirp signal was ≈ 2.4 s, so the data were overlapped by the total filter impulse response time of ≈ 15.6 s (155 072 samples)

giving a filter output duration of ≈ 10.85 s/segment. Since the process of bringing the optical cavities into resonance (lock) excites vibrations in the suspension wires, we discarded the first three minutes of data after each lock acquisition, allowing the vibrations to damp below other noise sources. Of the 39.9 locked hours of data, 8.8 h were in intervals too short to analyze; 111 locked intervals remained. Discarding the startup transient impulse response of the filters and the first three minutes of lock yielded $39.9 - 8.8 - 6.0 = 25.0$ h of data analyzed, in 8289 intervals of filter output (top of Fig. 1).

Poorly understood, nonstationary noise events corrupt the data. However, these transient events do not have the time-frequency behavior of inspiral chirps, so we can use the broadband nature of the interferometric detector to reject them. These events are discriminated from chirps by a χ^2 time-frequency test (Sec. 5.24 of Ref. [13]). The frequency band (dc to Nyquist) is divided into p subintervals, chosen so that, for a chirp superposed on Gaussian noise with the observed power spectrum, the expected contribution to ρ is equal for each subinterval. One forms a statistic χ^2 by summing the squares of the deviations of the p signal values from the expected value for the two template polarizations. We choose $p = 20$ so that Galactic signals that fall at the maximal template mismatch would not be rejected. In the presence of Gaussian noise plus chirp the statistic has a χ^2 distribution with $2p - 2 = 38$ degrees of freedom [13].

Occasionally, there are short sections (i.e., glitches) in the data when the instrument's output significantly exceeds the rms value. Some of these glitches were seismically induced. These short sections cause the outputs of the optimal filters to ring, but do not resemble binary inspiral chirps and are uniformly rejected by the time-frequency technique described above. However, these glitches bias $S_v(|f|)$ enough to create nonoptimal filters. To prevent this problem we estimate the power spectrum by averaging it for the eight glitch-free segments closest in time to the section being analyzed. The glitches were identified by seeing if too many samples fell outside a $\pm 3\sigma$ range or any fell outside a $\pm 5\sigma$ range. The number of segments (eight) was chosen to reduce the variance of the spectrum while still tracking changes in instrument performance.

The data was processed in about 32 h of clock time on a 48 node Beowulf computer at UWM (29 Gflops peak). The output of the filtering process is a list of signals for each segment j : the maximum (over t) SNR obtained for each filter k in the bank of 687 filters, the time t_j at which that maximum occurred, the value of the χ^2 statistic for that filter, and $N^{s.c.}$. In a given segment of data, we say that an event has occurred if the maximum SNR, over all filters for which the statistic χ^2 lies below some threshold χ_*^2 , exceeds a threshold ρ_* . The total number N of events observed in the data set of Fig. 1 is plotted as a function of these thresholds in Fig. 2.

Without operating two or more detectors in coincidence, it is impossible to characterize the non-Gaussian

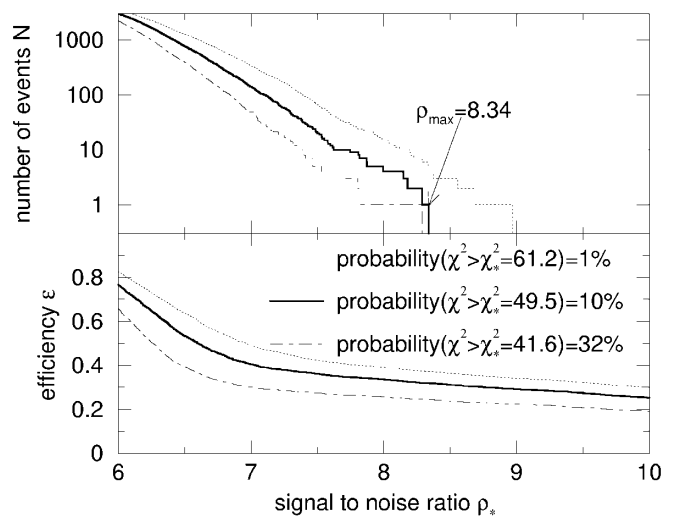


FIG. 2. Top: total number N of events observed, as a function of the SNR threshold ρ_* and the threshold χ_*^2 . Bottom: fraction ϵ of Galactic inspiral chirp signals that would lie above SNR threshold ρ_* and below χ_*^2 threshold χ_*^2 .

and nonstationary background well enough to state with confidence that an event has been detected. However one may estimate upper limits on the rate of Galactic neutron star binary inspirals (Poisson distributed in time) using a method which requires minimal assumptions about detector noise. Our limit $R_{90\%}$ is based on the probability of a Galactic neutron star binary signal having a SNR as big as the largest SNR observed. If the actual inspiral rate is greater than $R_{90\%}$ then it is likely that we would have observed a larger SNR event. Figure 1 shows that much of the time the detector was not pointing at the Galactic bulge; therefore the detector was only sensitive to a fraction of Galactic binary inspirals. Thus the event-rate bound depends on two numbers: (i) the efficiency ϵ_{\max} with which the instrument and filtering/analysis process can detect a binary inspiral in the Galaxy at the SNR ρ_{\max} of the largest observed event, and (ii) the total length $T = 25.0$ h of filtered data.

We determined the efficiency ϵ by Monte Carlo simulation, doing additional runs through the data set, and adding simulated Galactic inspiral waveforms [convolved with the detector response function $\tilde{R}(f)$] at 30 s intervals into the detector output $v(t)$. This allows us to characterize the detection process with the properties of the real instrument noise rather than an ad hoc model. The inserted waveforms were drawn from a population of binary neutron stars with a spatial number distribution given by $dN \propto e^{-D^2/2D_0^2} \mathcal{D} d\mathcal{D} \times e^{-|Z|/h_Z} dZ$, where \mathcal{D} is galactocentric radius, $D_0 = 4.8$ kpc, Z is height off the Galactic plane, and $h_Z = 1$ kpc is the scale height. This distribution is similar to the one presented in Ref. [14]. The detection efficiency ϵ is the fraction of these simulated inspirals which registered as events in our filtering/analysis procedure; it increases as the SNR threshold ρ_* is decreased, or as χ_*^2 is increased, and is shown in Fig. 2 for

the most-probable mass range [15] of $1.295M_{\odot}$ to $1.45M_{\odot}$ (the results depend weakly on the mass).

Our analysis gives an event-rate bound. With 90% confidence, the rate of binary inspirals in our Galaxy is less than $R_{90\%} = 3.89/[T\epsilon(\rho_{\max}, \chi_{*}^2)]$, where $\rho_{\max} = 8.34$ is the largest SNR event observed, and the threshold $\chi_{*}^2 = 49.5$ is chosen so that there is a 10% chance of rejecting a real chirp signal in stationary Gaussian noise. (This is a Bayesian credible interval computed using a “uniform prior” for the event rate. The dimensionless numerator depends only on the confidence level.) The efficiency $\epsilon(8.34, 49.5) = 0.33$ gives $R_{90\%} = 0.5 \text{ h}^{-1}$. This is a 90% confidence limit if the largest event is a real binary inspiral event. If the largest event is noise, the confidence is $\geq 90\%$. Thus, $R_{90\%}$ gives a conservative upper limit on the event rate when the detector noise is poorly understood. [The on-site environmental monitors show that some of the larger events in Fig. 2 arise from seismic disturbances or laser power fluctuations, but the largest event (on which our rate limit is based) was detected during normal instrument operation.]

Let us compare our limit $R_{90\%} = 0.5 \text{ h}^{-1}$, with the limit that could be obtained from the ideal analysis of an instrument that could detect every Galactic event. Operating for the same total time $T = 25.0 \text{ h}$ with an efficiency $\epsilon = 1$, the limit obtained would be 3 times better: $R_{90\%} = 0.17 \text{ h}^{-1}$.

Using stellar population models [16], one can forecast an expected inspiral rate of $R \sim 10^{-6} \text{ yr}^{-1}$, far below our limit. However, unlike these model-based forecasts, our inspiral limit is based on direct observations of inspirals. Our study also demonstrates methods being developed to analyze data from the next generation of instruments.

A previous search using 100 h of coincident Glasgow/Garching interferometer data gave an upper limit on burst sources [17]. The current generation of resonant-mass detectors [18] has established upper limits on monochromatic signals and stochastic background, but neither search addressed the binary inspiral rate. A coincidence analysis of bar data for coalescing binaries might produce a stronger limit than ours.

The full-scale 4-km LIGO interferometers will be much more sensitive than the 40-m prototype. Comprehensive instrument monitoring will permit detailed characterization of instrument anomalies and removal of some environmental noise. Correlation between three independent instruments will provide lower false alarm rates and greater statistical confidence. This will augment the techniques used here and allow LIGO to detect sources, as well as set tight rate limits. For example, if the largest coincident event detected by the LIGO interferometers has a SNR $\rho_{\max} = 5.5$, then we would obtain the limit

$$\mathcal{R}_{90\%} = 6 \times 10^{-5} \text{ Mpc}^{-3} \text{ yr}^{-1} \left(\frac{55 \text{ Mpc}}{r_{\max}} \right)^3 \left(\frac{1 \text{ yr}}{T_{\text{obs}}} \right),$$

on the rate of inspiral in the universe, where T_{obs} is the observation time, and r_{\max} is the distance to an optimally

oriented source with SNR $\rho_{\max} = 5.5$. For the initial LIGO interferometers, the distance is $r_{\max} = 55 \text{ Mpc}$; it will be 10 times larger for the enhanced interferometers, giving an expected rate limit of $6 \times 10^{-8} \text{ Mpc}^{-3} \text{ yr}^{-1}$. These limits should be compared to the best guess rate of $8 \times 10^{-8} \text{ Mpc}^{-3} \text{ yr}^{-1}$ given by Phinney [16].

We thank the LIGO project for making their data and resources available, and A. Abramovici, R. Spero, and M. Zucker for their contributions. P.R.B. thanks the Sherman Fairchild Foundation for financial support. J.D.E.C. was supported in part by NSERC of Canada. B.A. thanks B. Mours and his VIRGO colleagues for their assistance, and B. Barish, A. Lazzarini, G. Sanders, K. Thorne, and R. Weiss for helpful advice. This work was supported by NSF Grants No. PHY9210038, No. PHY9407194, No. PHY9424337, No. PHY9507740, No. PHY9514726, No. PHY9603177, No. PHY9728704, and No. PHY9900776.

-
- [1] A. Abramovici *et al.*, *Science* **256**, 325 (1992).
 - [2] See B. Caron *et al.*, in *Gravitational Wave Experiments*, edited by E. Coccia, G. Pizzella, and F. Ronga (World Scientific, Singapore, 1995); K. Danzmann *et al.*, *ibid.*; K. Tsubono *et al.*, *ibid.*
 - [3] R. John Sandeman, in *Second Workshop on Gravitational Wave Data Analysis*, edited by M. Davier and P. Hello, (Éditions Frontières, Paris, 1998).
 - [4] P.R. Saulson, *Fundamentals of Interferometric Gravitational Wave Detectors* (World Scientific, Singapore, 1994).
 - [5] T.T. Lyons, Ph.D. thesis, California Institute of Technology, 1997; A.D. Gillespie, Ph.D. thesis, California Institute of Technology, 1995; S. Smith, Ph.D. thesis, California Institute of Technology, 1988.
 - [6] A. Abramovici *et al.*, *Phys. Lett. A* **218**, 157 (1996).
 - [7] C. Cutler and É.É. Flanagan, *Phys. Rev. D* **49**, 2658 (1994); R. Balasubramanian, B.S. Sathyaprakash, and S.V. Dhurandhar, *Phys. Rev. D* **53**, 3033 (1996); *ibid.* **54**, 1860(E) (1996).
 - [8] L. Blanchet, B.R. Iyer, C.M. Will, and A.G. Wiseman, *Classical Quantum Gravity* **13**, 575 (1996), and references therein.
 - [9] S. Droz and E. Poisson, Sec. 6 in Ref. [13]; S. Droz, *Phys. Rev. D* **59**, 064030 (1999).
 - [10] B. Allen and P. Brady, Report No. LIGO-T970128-01-E, 1997 (unpublished).
 - [11] Robert Spero, Report No. LIGO-T970232-00-R, 1997 (unpublished).
 - [12] B.J. Owen, *Phys. Rev. D* **53**, 6749 (1996).
 - [13] B. Allen *et al.*, *GRASP: a Data Analysis Package for Gravitational Wave Detection*, version 1.8.4. Manual and package at <http://www.lsc-group.phys.uwm.edu>.
 - [14] S.J. Curran and D.R. Lorimer, *Mon. Not. R. Astron. Soc.* **276**, 347 (1995).
 - [15] L.S. Finn, *Phys. Rev. Lett.* **73**, 1878 (1994).
 - [16] E.S. Phinney, *Astrophys. J.* **380**, L17 (1991).
 - [17] D. Nicholson *et al.*, *Phys. Lett. A* **218**, 175 (1996).
 - [18] P. Astone *et al.*, *Astropart. Phys.* **7**, 231 (1997); P. Astone *et al.*, *Phys. Lett. B* **385**, 421 (1996); E. Maucelli *et al.*, *Phys. Rev. D* **56**, 6081 (1997).